

Two-Frequency Planar Doppler Velocimetry (2-n-PDV)

Tom O. H. Charrett, Helen D. Ford, David S. Nobes and Ralph P. Tatam⁽¹⁾

Optical Sensors Group, Centre for Photonics and Optical Engineering, School of Engineering, Cranfield University, Cranfield, Bedford, MK43 0AL, UK.

⁽¹⁾E-mail: r.p.tatam@cranfield.ac.uk

A Planar Doppler Velocimetry (PDV) system has been designed which is able to generate two beams, separated in frequency by 690 MHz. This allows a common-path imaging head to be constructed, using a single imaging camera instead of the usual camera pair. Both illumination beams can be derived from a single laser and acousto-optic modulators are used to affect the frequency shifts.

One illumination frequency lies on an absorption line of gaseous iodine, and the other in a region of zero absorption. The beams sequentially illuminate a plane within a seeded flow and Doppler-shifted scattered light passes through an iodine vapour cell onto the camera. The beam that lies in a zero absorption region is unaffected by passage through the cell, and provides a reference image. The other beam, the frequency of which coincides with an absorption line, encodes the velocity information as a variation in transmission dependent upon the Doppler shift. Images of the flow under both illumination frequencies are formed on the same camera, ensuring registration of the reference and signal images. This removes a major problem of a two-camera imaging head, and cost efficiency is also improved by the simplification of the system. The dual illumination technique has been shown to operate successfully with a spinning disc as a test object. Measurements have also been made on an axisymmetric air jet, Figure 1, for maximum velocities of $\sim 100 \text{ms}^{-1}$. A comparison with data obtained simultaneously, using a conventional two camera PDV arrangement has been made and the difference between the measurements found to be within a few m/s.

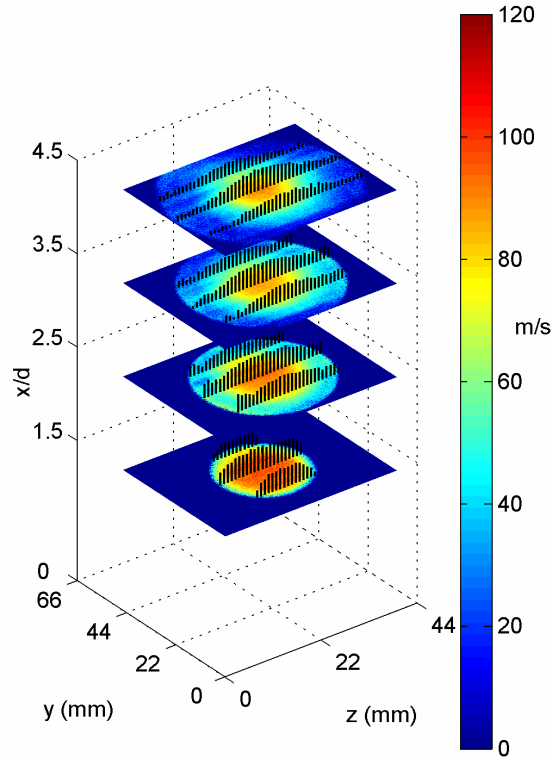


Fig 1: The velocity field of an axis-symmetric air jet calculated using the 2v-PDV system. Measurements were taken at 1.5, 2.5, 3.5 and 4.5 diameters downstream from the nozzle. Overlaid are vectors showing the magnitude of the velocity at various points (arrow heads have been removed for clarity)

1. Introduction

Planar Doppler Velocimetry (PDV) (Komine et al., 1991; Meyers, 1995; Irani & Miller, 1995; Ford & Tatam, 1997), also called Doppler Global Velocimetry (DGV), is a flow measurement technique that provides velocity information over a plane defined by a laser light sheet. PDV relies upon measuring the Doppler frequency shift of light scattered from particles entrained in the flow. As PDV relies upon the Doppler shift a single observation direction can measure a single component of velocity, as shown in Figure 2.

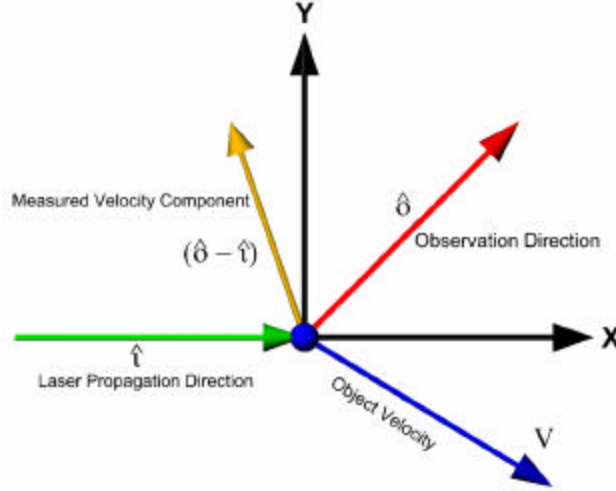


Fig 2: The relationship of laser illumination direction and observation direction to the measured velocity component determined from the Doppler equation.

The optical frequency shift, $\Delta \nu$, is given by the Doppler equation,

$$\Delta \nu = \frac{\nu(\hat{o} - \hat{i}) \cdot \mathbf{V}}{c} \quad (1)$$

Where ν is the optical frequency, \hat{o} and \hat{i} are unit vectors in the observation and illumination directions respectively, \mathbf{V} is the velocity vector and c is the free space speed of light.

The optical frequency of light scattered from each particle in the seeded flow experiences a Doppler shift, which is linearly related to the velocity of the particle at that point in the flow. In PDV, a region of the illuminated flow is imaged, through a glass cell containing iodine vapour, onto the active area of a CCD camera. Iodine has numerous narrow absorption lines over a large part of the visible spectrum (Gerstenkorn & Luc, 1986; Chan et al., 1995). If the laser frequency is chosen to coincide with one such line, the optical intensity at any position in the camera image is a function of the Doppler shift experienced at the corresponding flow position, via the frequency-dependent iodine absorption.

The intensity over a PDV image is affected by the intensity profile of the illuminating laser sheet (typically Gaussian), spatial variations of the seeding density within the flow, and diffraction fringes caused by imperfections in the optical surfaces. These variations are generally of similar amplitude to those resulting from absorption in the iodine cell, and can obscure the information about flow velocity that is contained within the camera image. It is therefore usual to amplitude-divide the image beam onto two cameras; from one of the two imaging paths the iodine cell is omitted, and the resulting image acts as a reference to normalize the signal image carrying the velocity information. This arrangement is shown in Figure 3(a).

Superposition of the reference and signal images to sub-pixel accuracy is essential if errors in the calculated velocities are to be minimized, for example Thorpe et al (Thorpe et al., 1995) assess the impact of image misalignment, on the velocity field of a rotating disc. For an image misalignment of 0.1 pixels, they give an estimate of this error as $\pm 5 \text{ ms}^{-1}$. Errors due to poor image registration can become particularly troublesome if large velocity gradients are present in the region imaged. The main causes of poor image registration are differences between the optical aberrations and magnifications of the two imaging paths. Thus errors tend to

be worse towards the outside edges of the images, where these factors are largest. Software de-warping routines can improve pixel matching (Reinath, 1997; Nobes et al., 2004b) and can help to correct for small differences in magnification. Post-processing cannot, however, correct for the almost inevitable differences in the optical distortions.

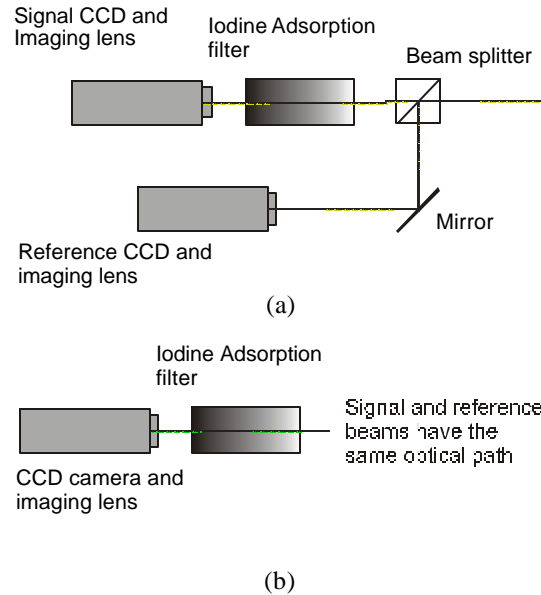


Fig 3: (a) Configuration of a conventional reference and signal camera PDV imaging arrangement used to measure a single component. (b) Configuration of a 2v-PDV system using a single camera.

Another potential source of error in a conventional PDV system is introduced by the use of a beam splitter. Ideally this would be completely insensitive to the polarization state of the scattered light, splitting the incoming light 50:50 between the signal and reference cameras. However even “non-polarizing” beam splitters retain a slight sensitivity to polarization, this can result in differing split ratios for different polarizations of light causing significant errors in the calculated velocities (Meyers & Lee, 2000). For example non-polarizing beam splitters are often quoted as $\pm 3\%$ variation in the split ratio for S and P polarized light, leading to typical velocity errors of $\pm 7\text{ms}^{-1}$.

One research group (Arnette, 2000) has attempted to address the problems identified. They used a single detector and two laser sources: a signal source tuned onto the slope of an iodine absorption band from an Nd:YAG laser at 532nm and a reference source from a Nd:YAG pumped dye laser at 618nm. The two signals were captured in one image on a single colour CCD camera. A data point was made up from the signal from a group of three pixels, one each measuring red, blue and green colours in the visible spectrum. The signal was collected on the green pixels while the reference was collected by the red pixels in each group. The significant advantage of this technique over the conventional PDV technique was the removal of the second reference camera as shown in the schematic of the two-frequency PDV detection head in Figure 3(b). The aim of this arrangement was to allow direct division of the captured images without image warping to get good image overlap. However the arrangement of pixels in a colour camera would imply that there is an image offset of at least one and possible two pixels between the signal and reference image. They also found that “signal bleed” of the scattered intensity from one pixel to another led to significant errors. It is also unclear what effect the absorption bands in the region of the 618nm reference beam had on the reference signal, as the iodine absorption spectrum was not reported either experimentally or theoretically at this wavelength. The effects of different scattering efficiencies of the particles at 532 and 618nm were not taken into account, nor were the differing responses of the CCD used at these different wavelengths. These are both potentially serious omissions as the Mie scattering for particles of a particular size varies by approximately 50% for a wavelength difference of approximately 90nm, at a centre wavelength of about 600nm, and this cannot be calibrated for practical systems.

This paper describes a technique termed two-frequency planar Doppler Velocimetry (2v-PDV), for overcoming these problems. The technique uses sequential illumination by optical beams, separated in frequency by 690 MHz but co-located in space. A reference beam is located in the non-absorbing section of the iodine transfer curve, and a signal beam is located on the slope of the absorption curve. Sequential illumination by each beam enables the reference and signal images to be acquired on the same CCD camera, avoiding image registration difficulties, to generate time-averaged velocity data.

2. Two-Frequency PDV (2v-PDV) – Principle of operation

The emission wavelength of the laser is tuned just off the low frequency side of an absorption line. The output beam is first frequency up shifted to lie in a zero absorption region of the iodine transfer function. A reference image is then acquired. The frequency is then downshifted to lie approximately midway (50%) on the iodine cell transfer function, see figure 4, and a signal image is acquired. The optical frequency difference is ~700MHz, which is sufficiently small that there will be no change in the scattering for the size of particles typically used; 0.2-5 μm diameter.

Exact alignment of the reference and signal images on the active area of the camera is automatic. The method also eliminates the polarization sensitivity of the split ratio of the beam splitter used in the two-camera system.

A potential limitation of the method described is that acquisition can no longer be perfectly simultaneous for the reference and signal images. Since the images are not spatially separated, they must instead be separated in time. For steady-state flows this is not a major difficulty, provided that the seeding is relatively dense and the seeding distribution remains essentially unchanged during the time taken to acquire the two image frames. The extent to which this condition is satisfied will depend upon the flow situation.

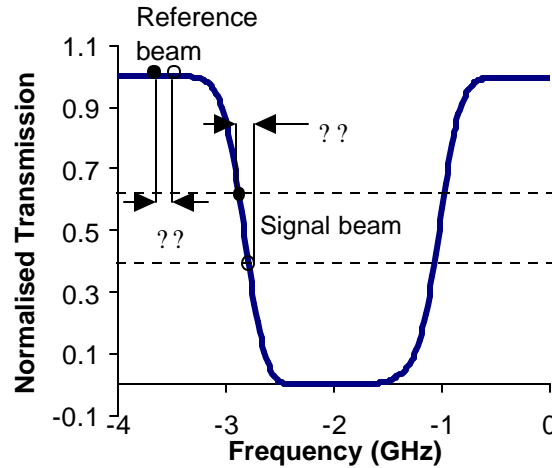
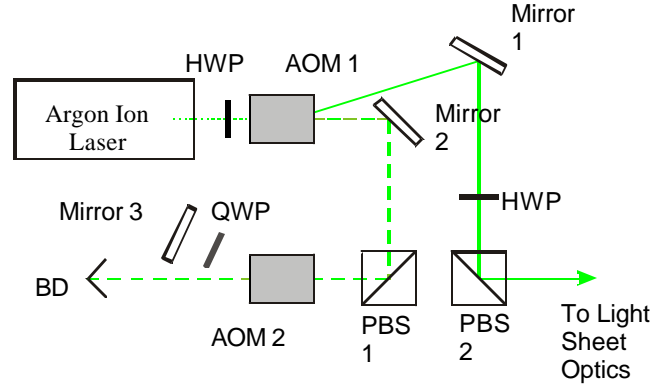


Fig 4: Relative positions of the laser frequency, and the shifted frequency on a typical absorption feature for 2v-PDV (Open circles denote the position of the illumination frequency and closed circles the Doppler shifted frequency.)

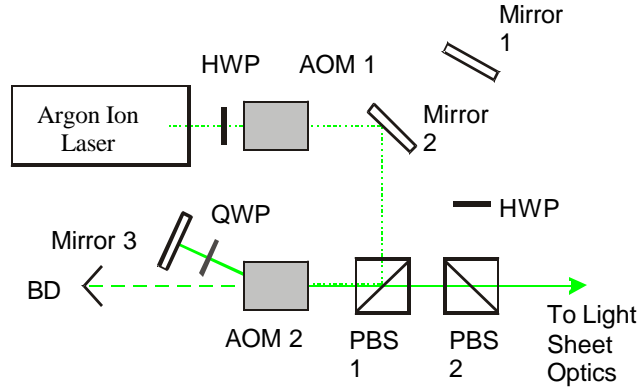
3. Experimental Arrangement

3.1. Illumination system

The light source was a tuneable Argon-ion laser (Spectra Physics Beamlok 2060), incorporating a temperature-stabilized etalon to ensure single-mode operation at 514.5 nm. The single-mode line width was about 2 MHz, which, as may be seen in section 3.2, is about three orders of magnitude lower than the width of the absorption line and can therefore be neglected in considering the absorption-related intensity variation. Optical frequency stability was about 3 MHz, plus a long-term drift with ambient temperature of about 40 MHz K^{-1} .



(a) The reference beam



(b) The signal beam

Fig 5: Schematic of the CW dual illumination PDV system

HWP - $\lambda/2$ plate; AOM – acousto-optic modulator; PBS – polarising beam splitter, QWP – $\lambda/4$ plate; BD – beam dump.

..... Laser Beam — Shifted Laser Beam. - - - Un-shifted Laser beam

The optical frequency of this light source was altered to form the reference and signal beams using a combination of two acousto-optic modulators. Figure 5 shows the configuration and operation of the dual illumination system. Figure 5(a) shows the beam path for the generation of the reference beam. The fundamental laser beam passes first through a half-wave plate (HWP) to adjust the polarization azimuth and then through an acousto-optic modulator, (AOM1). When AOM1 is switched on, the second order beam experiences a frequency shift of 170 MHz and is deflected through twice the Bragg angle. There is some loss of power as the process is not 100% efficient. Beam steering optics then redirect this beam into a position from which it can be coupled into a multimode optical fibre. The second half-wave plate, orientated so as to rotate the polarization azimuth through 90° , is necessary to achieve reflection of the beam at the polarizing beam splitter cube (PBS).

Conversely, when AOM1 is switched off, Figure 5(b), the signal beam is generated. The fundamental laser beam passes through with no frequency shift or angular deflection, and is incident upon a second mirror, which directs it into an alternative beam path. The beam passes through the active area of AOM2 and the optical frequency is altered by 260 MHz. The shifted beam is then retro-reflected by a mirror, making a double pass through a quarter wave plate (QWP), which rotates the polarization state by 90° . The beam makes a second transit through the AOM2, doubling the optical frequency shift to a total of ≈ 520 MHz, and is recombined with the reference beam in the output PBS and coupled into the same optical fibre as the reference beam.

In this work the beams are coupled into a multimode fiber and transported to a prism-scanning device. This scans the collimated beam rapidly across the region of interest, resulting in an ideal 'top-hat' intensity profile and avoiding the diffraction artifacts previously caused by imperfections in the sheet-forming optics (Roehle et al., 2000).

3.2. Image-capture system

As described in the introduction, the image-capture system can be greatly simplified compared with that required for a standard PDV system using a single illumination frequency. As both reference and signal beams pass through the iodine cell, the system is reduced to a single velocity component head consisting of a single solid state CCD camera, a zoom lens and a temperature-stabilized iodine cell positioned directly in front of the lens, as shown in Figure 3(b). However for this work it was decided to retain the conventional PDV head, Figure 3(a), with both signal and reference CCD cameras, as this allows the simultaneous collection of conventional PDV data when the flow is illuminated using the signal beam.

The cameras used for image capture were 'Imager Intense' cameras supplied by LaVision. These are digital cameras with 12 bit A/D conversion on a Peltier-cooled chip (-15°C), with a 1376 by 1040 image resolution. The pixel size is $6.7\mu\text{m}$ by $6.7\mu\text{m}$. Dedicated image acquisition and processing software (DaVis) is used to control the camera and to calculate and display normalized intensity maps. The integration time of the camera can be varied between 1 ms and 1000 s, depending on the scattered light intensity.

The iodine cell, which operates as a starved cell (Quinn & Chartier, 1993), is 25 mm in diameter and 50 mm long, with a cold finger. The use of a starved cell means that the control of the cell temperature can be less stringent, as above the starvation temperature all the iodine is in vapour form, so the characteristics of the absorption will not vary greatly with temperature fluctuations. The operating temperature should not be too much greater than the starvation temperature of the cell, otherwise thermal broadening of the absorption lines will alter the cell characteristics. The starvation temperature of the cell used is 40°C . The cold finger is held above this temperature using a Peltier element in a feedback loop, and the cell body is contained in an oven held at the same temperature (50°C).

Accurate velocity measurements using PDV require an exact knowledge of the shape of the iodine absorption line as a function of frequency. This was obtained by monitoring the intensity of a low-power beam, from the argon-ion laser, scattered off a surface and viewed using the PDV imaging head, as the laser frequency is scanned at a constant rate across the frequency range around the absorption line. The Spectra-Physics argon-ion laser used allows the optical frequency to be scanned by applying a voltage ramp to a modulation input that controls the etalon temperature. Because the optical frequency change is temperature based, it must be carried out slowly to avoid instability and mode hopping. An uninterrupted scan is generally difficult to achieve, so successive scans can be compiled to cover the full range. By passing the laser beam through an AOM and imaging the resultant different order beams, it was possible to measure the transmission at several frequencies simultaneously, and with a frequency spacing that is known. This allowed the easy identification of any mode hops, as well as providing a reference for the conversion from etalon voltage to frequency. The resultant compiled scan is shown, in figure 6, overlaid with the theoretical absorption spectrum, calculated using the (Forkey, 1996) model for our iodine cell.

The near-linear region between the normalized absorption values of 0.2 and 0.8 corresponds to a frequency range of about 300 MHz. For practical illumination/viewing geometries, this typically allows measurement of flow velocities from a few meters per second up to a few hundred meters per second. Measurement error, as a fraction of the measured value, is lower for higher flow velocities.

An important consideration that is unique to 2v-PDV is the shape of the absorption line in the region of zero absorption. As the reference image is captured using light with an un-shifted frequency, coinciding with the full transmission portion, any Doppler shifts caused by scattering in the flow, should cause no change in the level of light that is transmitted, for this reference to be true. The scans of the iodine cell show that the zero absorption region is constant, at full transmission, for approximately 0.8 GHz which would require typical velocity shifts of several hundred meters per second for the reference intensity to be affected by the iodine vapour.

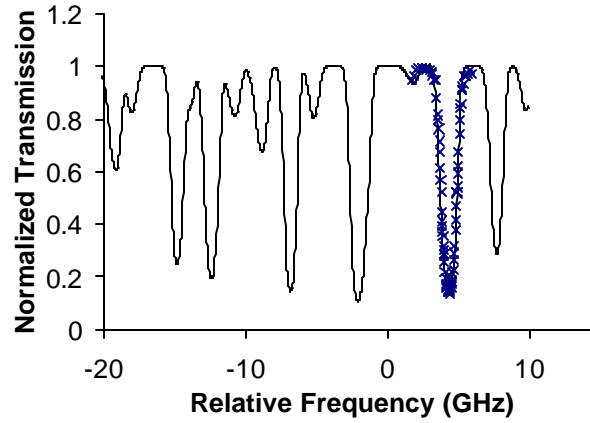


FIG. 6. Diagram showing the experimental iodine cell scan plotted over the theoretical absorption spectrum calculated using the Forkey's model.

3.3. Processing scheme

The collected data consisted of two pairs of images; one pair is captured with the flow illuminated by the reference beam, and the other with the flow illuminated by the signal beam. One image of each pair was viewed through the iodine cell, onto the signal CCD, whilst the optical path for the second image omitted the iodine cell and was imaged onto the reference CCD. It should be noted that only the first image of both pairs is necessary for the 2v-PDV technique described. However the simultaneous collection of the images from the reference CCD allows the data to be processed as in conventional PDV, for direct comparison with the 2v-PDV data. Although the beam splitter is still included in the experimental arrangement this did not affect the 2v-PDV results as the polarization state of the light scattered from the particles did not change during image acquisition.

In its simplest form, processing the images consists of a background subtraction to remove ambient scattered light and camera dark current (Elliott & Beutner, 1999). This background is typically obtained by averaging multiple background images, taken shortly before the acquisition of the raw data. This ensures that the ambient light level, geometry and laser power are identical to those during the data collection. This is followed by division of the signal image by the reference image, producing the normalized image that should contain the intensity variations caused by the Doppler shifts. Velocity is then calculated by de-convolution using the iodine absorption curve. Image de-warping is not essential, since image registration is automatic, and only a single component of velocity was measured.

Typically, the reference and signal illumination beams will be of different power, so a normalization factor was included to account for this in taking the ratio between the images. This factor was found by taking the ratio of the power in the signal and reference beams. It is also important to take background images for each illumination beam independently, because of the difference in the ambient scattered light caused by the different optical paths in generating the beams. As an additional stage the recorded images had a threshold applied to remove pixels with levels below, or above those that were considered reliable, for example to remove saturated pixels, outside the linear region of the CCD response, or those in which the signal level was too low to be reliable, typically < 100 counts.

4. Results

4.1. Measurements on a rotating disc

The first test object used to assess the system was a Perspex disc 150mm in diameter, coated with matt white paint, intended to give a near uniform reflection, and mounted centrally on the spindle of a rotary motor. The aim of this experiment was to investigate a known velocity field. The maximum circumferential velocity of the wheel was 31ms^{-1} . Figure 7(a) shows a representation of the experimental arrangement including the

swept light sheet generator (Roehle et al., 2000) and the Perspex disk. The observation direction was at an angle of 26° to the illumination direction from the centre of the disc to the centre of the CCD. The geometry was chosen to have a high sensitivity to the horizontal component of rotational velocity, which is expected to vary linearly along any vertical line through the disc.

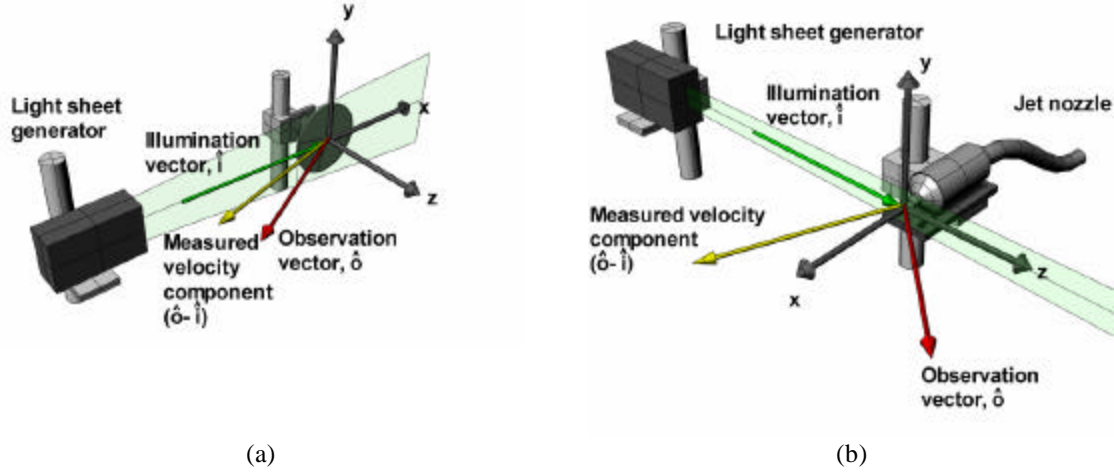


Fig 7: 3D representation of the experimental arrangements for (a) Wheel measurements and (b) Jet measurements

Sets of image pairs were stored for both anticlockwise and clockwise rotation of the disc, as viewed from the front, at the maximum rotation speed. The illumination intensity profile actually varied slightly for reference and signal illumination beams, possibly due to differences in the mode mixing within the multimode fibre. The fibre did not transmit a large number of modes, and the output mode pattern in this case is very sensitive to the optical coupling geometry at the fibre input. Because of the differing intensity profiles, a further processing step was required; a 'white card' image (Reinath, 1997) was taken for each illumination beam, with the laser tuned off the absorption line. This was used to normalize the individual signal and reference images.

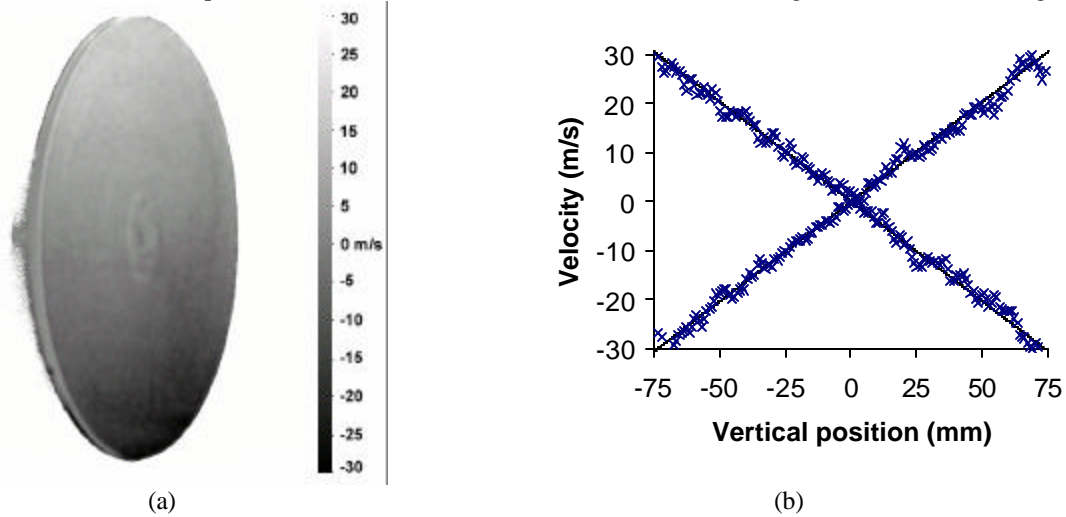


Fig 8: (a) A typical computed velocity field made using the single camera 2v-PDV system (b) Vertical profiles through the measured velocity field, for clockwise and anticlockwise rotation of the disc. The solid lines represent the theoretical velocity gradient (every 5th point shown).

A typical processed velocity field is shown in Figure 8(a). Profiles of the greyscale value were taken vertically through the smoothed images passing close to the centre of the disc. The profiles, for both clockwise and anticlockwise rotation, are shown in Figure 8(b), along with the theoretical velocity gradient. As expected, the velocity gradient is negative for the first plot, and positive for the second, corresponding to the reversal in the sense of rotation. The velocity error for these plots is about $\pm 2 \text{ ms}^{-1}$.

4.2. Measurements on a circular jet

Measurements were carried out on an axis-symmetric air jet, with a 20mm diameter smooth contraction nozzle. The air intake to the jet was seeded using a Concept Engineering ViCount compact smoke generator, which produces particles in the 0.2-0.3 μ m diameter range. Figure 7(b) shows the experimental arrangement with the main flow direction of the jet perpendicular to the laser sheet. The observation direction was placed in forward scatter where scattering intensities are greatest; this results in a measured velocity component that is $\sim 20^\circ$ from the main jet velocity component. The jet has a theoretical exit velocity of 94ms⁻¹, which was calculated by measuring the nozzle pressure ratio. Sets of image pairs were captured at various positions downstream from the nozzle; this was achieved by moving the nozzle position, in the x direction, relative to the laser sheet. Again the optical power at the output of the optical fibre was about 5 mW, and the integration time on the cameras was 10-15 s.

The velocity field at each position, 1.5, 2.5, 3.5 and 4.5 nozzle diameters downstream are shown as a 3-dimensional representation in Figure 1.

Differences in illumination intensity profiles for the reference and signal illumination beams were again present but as the laser sheet used for the jet was small and well-focused, compared to the thick sheet used with the wheel, it was no longer necessary to apply the 'white card' correction.

The 2v-PDV results were compared with a conventional two-camera arrangement by using the second camera in the PDV head to simultaneously capture standard PDV data. This was processed using images captured when the signal beam was illuminating the flow, with the second camera providing the reference image. When the standard PDV data was processed it was necessary to apply a 'white card' correction. The need for this correction has also been observed in our previous work, as well as by other researchers (Reinath, 1997; Elliott & Beutner, 1999; McKenzie, 1997).

A comparison of profiles through the centre of each slice, for the 2v-PDV (single CCD) and standard (two CCD) PDV jet measurements can be seen in figure 9 along with the theoretical velocity. The results from the two techniques agree well to within $\sim \pm 5\text{ms}^{-1}$ over most of the jet diameter, although the difference is greater towards the edges of the jet. This can be accounted for by lower signal levels caused by less seeding present in this region of the jet.

5. Discussion

The processing is made extremely straightforward in the single camera system, by the avoidance of any pixel-matching requirement between the signal and reference images. This can be demonstrated by the fact that a 'white card' correction was not necessary when processing 2v-PDV results for the seeded flow, but was necessary when processing the conventional, two camera, PDV results for the same flow, collected simultaneously.

Careful coupling of the two beams into the multi-mode fibre is necessary to ensure that the spatial profile for both the signal and reference beams are similar. If these differ significantly, the illumination profiles can also differ, especially when a thick sheet is required, such as when illuminating the face of disc. This resulted in the need for the 'white card' correction in both the 2v-PDV and standard two camera PDV measurements on the disc.

The power available at the output of the multimode fibre is currently about 48 mW from a laser output of about 700 mW, which although inefficient, is sufficient for making measurements at integration times of a few tens of seconds. A significant amount of power is lost because the optical arrangement includes many surfaces, few of which are anti-reflection coated at 514 nm. Efficiency would be improved by substituting coated optics. The major losses however occur in the particular AOMs used. The 260 MHz AOM has a very small aperture and a first-order efficiency of less than 50%, and two passes are made through this component. Up to ten times more power is available in the reference beam path, since the 85 MHz AOM has a much larger aperture and is more efficient. Components are now available with improved efficiencies and offering larger optical frequency shifts, so we expect to be able to improve the available power from the system to a

level more usable in real flows. For example, using two 350 MHz AOMs in single pass, at least an order of magnitude improvement in delivered power would be expected; possibly up to two orders of magnitude, which would result in 100-200 mW in the measurement volume.

An additional increase in illumination intensity could be obtained by scanning the laser beam across a smaller measurement volume.

Future improvements in the sensitivity of the 2ν -PDV technique could be carried out by tuning both frequencies to positions on the iodine absorption line, with the first at the 50% position on the down slope, and the second similarly positioned on the upslope. A Doppler shift resulting from the measured flow will decrease the transmission of one beam whilst increasing the transmission of the other, potentially doubling the sensitivity. It would be necessary to take account of the differing gradients of the two slopes, as well as the

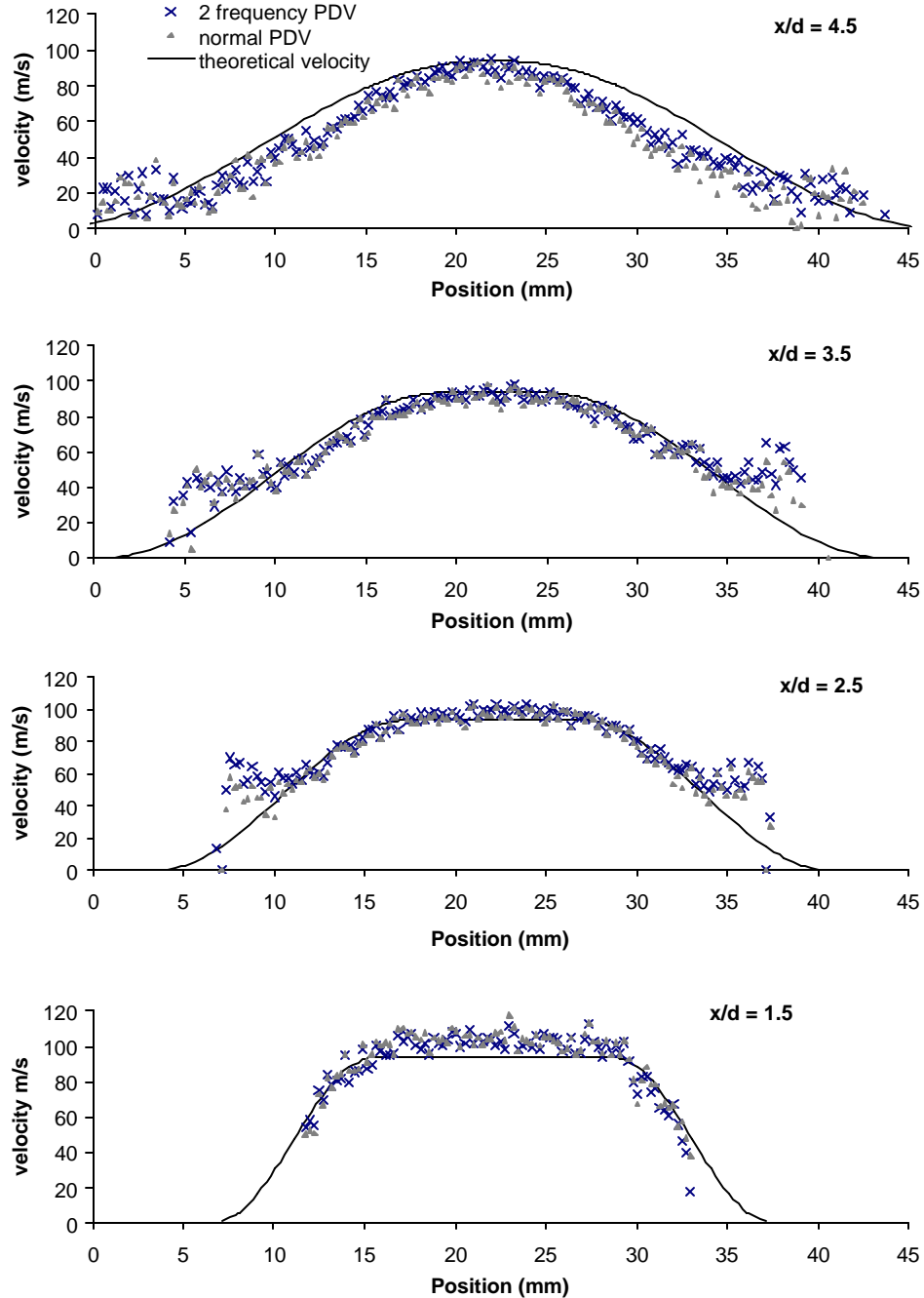


Fig 9. A comparison between profiles, taken through the centre of the air jet at 1.5, 2.5, 3.5 and 4.5 diameters downstream, for the 2ν -PDV (single CCD) and standard (two CCD) PDV results (every 5th point shown) and the theoretical jet profile.

exact level of transmission for each un-shifted frequency. This was not attempted here, as the separation between the two beams would have to be greater than the 690MHz that was available, so that both beams can be positioned on the linear portions of their respective slopes. However, the use of higher frequency AOMs will enable investigation of this approach.

An innovative three-component PDV system has been developed at Cranfield under a separate programme (Nobes et al., 2004a; Nobes et al., 2003), using a coherent optical fibre bundle to transmit three views of the flow, monitored from different viewpoints, back to the camera. The small size of the bundle means that it is still possible to operate with a single camera and cell, while now obtaining full three-component flow information. The bundle-based viewing system can be used with the dual illumination configuration to obtain three-component data, provided that sufficient optical power is available, from a single CCD camera.

6. Conclusions

It has been shown that a PDV illumination system using dual-frequency illumination generated by two acousto-optic modulators, and optical fibre-delivered to the measurement region, can eliminate one of the cameras from the conventional Planar Doppler Velocimetry (PDV) sensing head. Automatic superposition of the signal and reference images is achieved, and polarization errors caused by the beam splitter in the conventional system are eliminated. The system has been tested on a rotating wheel, and is currently achieving a velocity resolution of about $\pm 2 \text{ ms}^{-1}$, limited by the quality of the light sheet generated from the multimode fibre. Measurements have also been made on a circular air jet, and a comparison with standard (two CCD) PDV results, captured simultaneously has been made which showed good agreement to within a few m/s.

Acknowledgments

This work was supported by the Engineering and Physical Sciences Research Council (EPSRC) UK, under grant GR/S04291, and the Royal Society UK. HDF acknowledges a Daphne Jackson Fellowship funded by the Royal Academy of Engineering.

References

- Arnette, S. A. (2000). "Two-Color Planar Doppler Velocimetry", *AIAA Journal*, Vol. 38, No. 11, pp 2001-2006.
- Chan, V. S. S., Heyes, A. L., Robinson, D. I., and Turner, J. T. (1995). "Iodine Absorption Filters for Doppler Global Velocimetry", *Measurement Science and Technology*, Vol. 6, pp 784-794.
- Elliott, G. S. and Beutner, T. J. (1999). "Molecular Filter Based Planar Doppler Velocimetry", *Progress in Aerospace Sciences*, Vol. 35, pp 799-845.
- Ford, H. D. and Tatam, R. P. (1997). "Development of Extended Field Doppler Velocimetry for Turbomachinery Applications", *Optics and Lasers in Engineering*, Vol. 27, pp 675-696.
- Forkey, J. N. (1996). "Development and Demonstration of Filtered Rayleigh Scattering - a Laser Based Flow Diagnostic for Planar Measurements of Velocity, Temperature and Pressure", *Final Technical Report for NASA Graduate Student Researcher, Fellowship Grant #NGT-50826*, Princeton University.
- Gerstenkorn, S. and Luc, P. (1986). "Atlas du Spectre d'Absorption de la Molecule d'Iode 14800-200 cm^{-1} Complement: Identification des Transitions du Systeme (B-X)", *Laboratoire Aime-Cotton, Centre Nationale de la Recherche Scientifique*, Orsay, France.
- Irani, E. and Miller, L. S. (1995). "Evaluation of a Basic Doppler Global Velocimetry System", *Society of Automotive Engineers*, Paper 951427.

- Komine, H., Brosnan, S., Litton, A., and Staeppeerts, E. (1991). "Real-Time Doppler Global Velocimetry", *AIAA 29th Aerospace Sciences Meeting*, Reno, Nevada, Paper 91-0337.
- McKenzie, R. L. (1997). "Planar Doppler Velocimetry Performance in Low-Speed Flows", *35th AIAA Aerospace Sciences Meeting and Exhibit*, Reno, Nevada, AIAA 97-0498.
- Meyers, J. F. (1995). "Development of Doppler Global Velocimetry as a Flow Diagnostic Tool", *Measurement Science and Technology*, Vol. 6, pp 769-783.
- Meyers, J. F. and Lee, J. W. (2000). "Identification and Minimization of Errors in Doppler Global Velocimetry Measurements", *10th International Symposium on Applications of Laser techniques to Fluid Mechanics*, Lisbon, Portugal,
- Nobes, D. S., Ford, H. D., and Tatam, R. P. (2003). "Planar Doppler Velocimetry Measurements of Flows using Imaging Fiber Bundles", *Proc. SPIE*, 5191, pp 122-133.
- Nobes, D. S., Ford, H. D., and Tatam, R. P. (2004a). "Three Component Planar Doppler Velocimetry Using Imaging Fibre Bundles", *Experiments in Fluids*, Vol. 36, No. 1, pp 3-10.
- Nobes, D. S., Wieneke, B., and Tatam, R. P. (2004b). "Determination of View Vectors from Image Warping Mapping Functions", *Optical Engineering*, Vol. 43, pp 407-414.
- Quinn, T. J. and Chartier, J.-M. (1993). "A New Type of Iodine Cell for Stabilized Lasers", *IEEE Transactions on Instrumentation and Measurement*, Vol. 42, pp 405-406.
- Reinath, M. S. (1997). "Doppler Global Velocimeter Development for the Large Wind Tunnels at Ames Research Center", *NASA Technical Memorandum*, No. 112210.
- Roehle, I., Willert, C., Schodl, R., and Voigt, P. (2000). "Recent Developments and Applications of Quantitative Laser Light Sheet Measuring Techniques in Turbo machinery Components", *Measurement Science and Technology*, Vol. 11, pp 1023-1035.
- Thorpe, S. J., Ainsworth, R. W., and Manners, R. J. (1995). "The Development of a Doppler Global Velocimeter and its Application to a Free Jet Flow", *ASME / JSME Fluids Engineering and Laser Anemometry Conference and Exhibition*, Hilton Head, SC, USA,